

Research Article

Open Access

Antitumor Activity of Furanoallocolchicinoid-Chitosan Conjugate

Elena V Svirshchevskaya^{1*}, Iuliia A Gracheva², Andrey G Kuznetsov^{1,3}, Ekaterina V Myrsikova¹, Maria V Grechikhina¹, Anastasia A Zubareva⁴ and Alexey Yu Fedorov²

¹Shemyakin-Ovchinnikov Institute of Bioorganic Chemistry RAS, 16/10, Miklukho-Maklaya St., 117997, Moscow, Russian Federation

²Department of Organic Chemistry, Nizhni Novgorod State University, Gagarina av. 23, Nizhni Novgorod 603950, Russian Federation

³Moscow State University, Leninskie gory 1, 119991, Moscow, Russian Federation

⁴Institute of Bioengineering, Research Center of Biotechnology RAS, 33, bld. 2 Leninsky Ave., Moscow, Russian Federation

Abstract

Colchicine irreversibly binds to tubulin, blocks microtubule formation, and inhibits cell division. However, its usage as an antitumor agent is limited due to its distribution to many tissues and low accumulation in the tumor. The increase in molecule weight can change colchicine biodistribution and decrease side effects. The aim of this work was to study *in vivo* and *in vitro* antitumor activity of colchicine-chitosan conjugate. A new allocolchicine derivative – furanoallocolchicinoid **3** was synthesized and conjugated to chitosan (**4**). Both **3** and **4** induced *in vitro* tubulin reorganization, cell cycle arrest, and inhibition of cell proliferation in 2D and 3D cultures. Antitumor effect of chitosan, **3**, and **4** was studied in Wnt-1 breast tumor bearing mice. Conjugate **4** demonstrated significantly better tumor growth inhibition than **3** possibly as a result of a better accumulation in the tumor.

Keywords: Furanoallocolchicinoid; Chitosan; Multicellular tumor spheroids; Wnt-1 breast tumor

Introduction

Colchicine is a small 400 Da hydrophobic molecule which passively penetrates cells and irreversibly binds to β -tubulin by this mean preventing microtubule formation and cell division [1-4]. Modernly colchicine is approved by FDA for the treatment of acute gout and familial Mediterranean fever, Behcet disease, chondrocalcinosis, and other microcrystalline arthritis [5,6]. Potential indications include primary biliary cirrhosis, psoriasis, amyloidosis, various dermatitis, relapsing polychondritis, necrotizing vasculitis, Sweet's syndrome, leukocytoclastic vasculitis [7-9]. Due to its extremely specific antimitotic activity, colchicine can be a potent antitumor agent. High therapeutic doses (50-100 mg/m²) induce relatively mild side effects the commonest of which (5-10%) is general gastro-intestinal toxicity [10-12]. Earlier studies demonstrated that colchicine antineoplastic therapeutic index is narrow [11]. Besides, in rare cases on average well tolerated doses of colchicine can be lethal [10,13]. Modernly several clinical trials are being conducted to find safer protocols for mitotic inhibitors such as colchicine, vincristine, taxol, and others to treat advanced cancer [14-17].

Colchicine is a small hydrophobic molecule able to bind serum albumin and to accumulate in leukocytes [18,19]. Blood colchicine half-life was estimated as 17 hours and maximal blood concentration was found 2 h after injection [20]. Biodistribution studies were conducted 20 years ago by Mehta et al. using autoradiography [21] and recently by Erfani et al. [22]. The authors demonstrated that tumor/muscle ratio was around 4 at 1 h after injection [21-22]. This is relatively high however, liver, intestine, kidney, and heart accumulated colchicine at ratios 11, 5, 7, and 6 accordingly [21] showing that the major obstacle is a high accumulation of colchicine in non-target organs. Close data were obtained by Satpati et al. who showed tumor/blood and tumor/muscle ratios 0.14 and 1 at 1 h after injection that increased to 1 and 4 at 24 h accordingly [20]. Colchicine as well as other hydrophobic drugs is likely to have a high partition coefficient ($\log(P)$). For example, paclitaxel $\log(P)$ was >4 as determined by Colby et al. using dialysis partitioning experiments [23]. Most anti-microtubules have distribution coefficient $\log(D)$ from 2 to 7 [24]. This means that colchicine partitions quickly into adjacent cell membranes (lipophilicity), primarily binding blood leucocytes and lately – endothelial and epithelial cells.

Unspecific tissue partition of colchicine may be reduced by

decorating it with hydrophilic groups such as PEG [25]. Another way to sequester colchicine from non-target organs is to increase its molecular weight (MW) [25]. Indeed, the increase in the molecule size can improve the therapeutic index of anticancer agents *via* “enhanced permeability and retention effect” [26] due to an increased uptake of macromolecules by tumors.

Drug conjugates are intensively studied. The concept of “smart” antitumor drug conjugate was first proposed by Ringsdorf [27]. The Ringsdorf model implies a conjugation of the drug to a biocompatible polymer backbone and additionally its decoration with a targeting moiety able to deliver the conjugate to a particular tumor associated target. Basing on Ringsdorf model multiple drug conjugates were developed. PEG is one of the most popular polymers used to reduce hydrophobicity and to increase MW of many antitumor drugs including colchicinoids [28-32]. Besides, PEG also shields colchicine from interactions with plasma albumin. Of note, the only nanosized drug conjugate with anti-microtubule agent recommended for the treatment of metastatic breast cancer – Abraxane, is paclitaxel-albumin nanoparticles [33]. The results of *in vivo* studies demonstrate that drug conjugates better accumulate in tumors and induce fewer side effects [28-35].

However, PEG molecule possesses only one reactive group which can be used for conjugation. It makes it difficult to equip the conjugate with a targeting group as well as to immobilize several molecules of a drug on the long polymeric backbone.

Among many biodegradable and biocompatible polymers, chitosan and its derivatives are ones of the best. Chitosan is a biodegradable nontoxic polycation with multiple reactive groups easily used to obtain derivatives with a desired charge and hydrophobic properties

***Corresponding author:** Shemyakin-Ovchinnikov, Institute of Bioorganic Chemistry RAS, 16/10, Miklukho-Maklaya St., 117997, Moscow, Russian Federation, Tel: +74953304011; E-mail: esvir@mx.ibch.ru

Received September 02, 2016; **Accepted** September 20, 2016; **Published** September 23, 2016

Citation: Svirshchevskaya EV, Gracheva IA, Kuznetsov AG, Myrsikova EV, Grechikhina MV, et al. (2016) Antitumor Activity of Furanoallocolchicinoid-Chitosan Conjugate. Med Chem (Los Angeles) 6: 571-577. doi:10.4172/2161-0444.1000401

Copyright: © 2016 Svirshchevskaya EV, et al. This is an open-access article distributed under the terms of the Creative Commons Attribution License, which permits unrestricted use, distribution, and reproduction in any medium, provided the original author and source are credited.

[36]. Unmodified chitosan is soluble in diluted acids and aggregates at neutral pH. Substitution of amino groups for carboxyl ones increases chitosan solubility at neutral pH while hydrophobic chitosan derivatives are prone to form nanoparticles spontaneously in aqueous solutions [37,38].

This study is designed as a “proof-of-concept” one. Recently we have synthesized a series of potent allocolchicine analogues - furanoallocolchicinoids [39]. In this work we tried to obtain a conjugate of furanoallocolchicinoid **2** [39] with 40 kDa chitosan and to study its *in vitro* and *in vivo* activity.

Materials and Methods

Materials

Medium molecular weight (MW) chitosan with deacetylation degree 0.94 (Aladdin Chemistry Co., Ltd., Shanghai, China); *N,N'*-carbonyldiimidazole (CDI) (Sigma); succinic anhydride (Pierce); 1-ethyl-3-[3-dimethylaminopropyl]-*N*-(3-dimethylaminopropyl)-*N'*-ethylcarbodiimide hydrochloride (EDC) (Pierce); *N*-hydroxysuccinimide (NHS) (Reanal) were used. Chitosan was purified by an extensive dialysis. All other chemicals were of analytical grade and used as received.

Methods

Dynamic Light Scattering (DLS): The average molecule size of **3** and **4** was determined using 90 Plus Particle Size Analyzer (Brookhaven, United States) in water ($25.0 \pm 0.1^\circ\text{C}$) at a scattering angle of 90° and wavelength of 661 nm using Big Particle Sizing Software. Zeta potential of NPs was determined in 10 mM KCl solution using identical Big Pal Zeta-Potential analyzer hard-ware and software.

MTT-assay: Cytotoxic effect of **1-4** derivatives was estimated by a standard 3-(4, 5-dimethyl-2-thiazolyl)-2, 5-diphenyl-2H-tetrazolium bromide (MTT, Sigma) test in 2 dimensional (2D) conditions as was described earlier [40,41]. To analyze the effect of the preparation in 3D conditions 96-flat bottom plates were coated with poly(2-hydroxyethyl methacrylate) (PolyHEMA, Sigma), cells were seeded and cultivated overnight to form 3D spheroids. Compounds **1-3** were dissolved in dimethylsulfoxide (DMSO) to 20 mM concentration and stored at -20°C until the assay. Solution of the conjugate **4** was either stored at $+4^\circ\text{C}$, frozen at -20°C or freeze-dried and stored at $+4^\circ\text{C}$. Specific activity did not depend much on the type of the storage (Table S1). Different dilutions of the compound **1-3** from 20 μM to 0.1 nM were prepared separately and transferred in 100 μl to the plates with the cells. Non-treated cells served as controls. Specific activity of **3** in the conjugate **4** solution was predetermined in 2D experiments. Plates were incubated for 72 h. All samples were run in three replicas and all experiments were repeated 2-3 times in each cell line. For the last 3-4 hours, 20 μl (5 mg/ml) of MTT was added to each well. Cytotoxic concentration giving 50% of the maximal toxic effect (IC_{50}) was calculated from the titration curves. The inhibition of proliferation (inhibition index, II) was calculated as $[1 - (\text{OD}_{\text{experiment}}/\text{OD}_{\text{control}})]$, where OD was MTT optical density.

Cell cultures: Colo-357, MiaPaCa-2, BxPC-3 pancreatic human adenocarcinoma cell lines, HaCaT noncancerous human keratinocytes, noncancerous endothelial cells EA.hy926, and Wnt-1 related murine epithelial cell line W1204, generated by us earlier [42], were used in the study. Human cells were grown in DMEM supplemented with 10% fetal calf serum (FCS), pen-strep-glut (all from PanEco, Moscow, Russian Federation). W1204 cells were grown in RPMI-1640 with the same supplements and 10E-5M 2-mercaptoethanol. Cells were

passaged by trypsinization using Trypsin/EDTA solution (PanEco, Moscow, Russian Federation) twice a week. Twenty four hours before the assays, cells were seeded in the appropriate plates adjusted to 3×10^5 cells/ml and incubated overnight to achieve standardized growth conditions. To prepare multicellular spheroids (3D cultures), plates (Costar, USA) were coated with pHEMA, dried, and used at request.

Confocal analysis: For confocal analysis cells were grown overnight on sterile cover slips in 200 μl of complete culture medium in 6-well plates (Costar). Allocolchicinoids were added to the wells at 4 μM and cells were cultivated for 72 h. After incubation cells were fixed with 1% paraformaldehyde, permeabilized by 0.1% Triton X100 in PBS, stained with anti- β -tubulin antibody (SantaCruz, USA) followed by anti-mouse-IgG-AlexaFluor594 (Molecular Probes, USA), washed and polymerized with Mowiol 4.88 medium (Calbiochem, Germany). Actin expression was analyzed by Phalloidin-AlexaFluor488 (Molecular Probes, USA) staining of permeabilized cells for 30 min. Hoechst 33342 (Sigma) was used to visualize nuclei. Slides were analyzed using Eclipse TE2000 confocal microscope (Nikon, Japan).

Cell cycle analysis: Cell cycle was analyzed using propidium iodide stained DNA. Cells were incubated with colchicine derivatives for 72 h in 2D or 3D conditions, trypsinized, washed in ice-cold PBS, fixed by 70% cold ethanol and left for 2 h at -20°C . Important, trypsinization of multicellular tumor spheroids was incomplete. Addition of collagenase A (Roche, USA) at 0.3 units/ml to trypsin/EDTA solution helped to obtain single cell suspension. Thereafter, the cells were washed twice in PBS, stained with 50 $\mu\text{g}/\text{ml}$ of propidium iodide (Sigma Chemical Co) in PBS, 10 $\mu\text{g}/\text{ml}$ of DNase and analyzed by flow cytometry using FACScan device (BD, USA). Cell cycle analysis was repeated multiple times with the same results. The results were analyzed using WinMDI 2.8 software.

In vivo experiments: C57BL/6 mice were purchased from Pushchino Affiliation of Shemyakin-Ovchinnikov Institute of Bioorganic Chemistry RAS, Moscow. All mice were 6–8 wk old and maintained in minimal pathogen animal facility at the Shemyakin-Ovchinnikov Institute of Bioorganic Chemistry RAS, Moscow. All studies were conducted in an AAALAC accredited facility in compliance with the PHS *Guidelines for the Care and Use of Animals in Research*. Wnt-1 tumor cells [42] ($10^6/\text{mouse}$) were obtained from a frozen stock, thawed and inoculated subcutaneously into the left inguinal mouse fat pad (MFP #4). The injection of cells in 100 μl of PBS was performed through the skin of anesthetized mice. Tumor size was measured with vernier calipers twice a week and calculated using the formula $(W^2 \times L)/2$, where W and L corresponded to width and length of tumors. Before the treatment, mice were sorted to obtain comparable average volume of tumors (50–200 mm^3) in all groups (n=4–5). Allocolchicine derivatives were injected in the dose 10 $\mu\text{g}/\text{mouse}$ (400 $\mu\text{g}/\text{kg}$) of colchicine equivalent in 200 μl of saline intravenously into the orbital sinus of mice at days 20, 25, 30, and 35. Control group was injected with saline only. Chitosan group was injected with 200 $\mu\text{g}/\text{mouse}$ of chitosan, which was an equivalent amount of chitosan in sample **4**. The experiment was terminated at day 40 when two control mice died.

Statistical analysis: Statistical analysis was performed using Student's t-test. Comparison values of $p < 0.05$ were considered statistically significant.

Experimental

Synthesis of allocolchicine derivatives

Furanoallocolchicinoid **2** (*N*-((1*S*)-2-(Hydroxymethyl)-1',2',3'-

trimethoxy-6,7-dihydro-*H*-benzo[5',6':5,4]cyclohepta[3,2-f]benzofuran-1-yl)acetamide) was synthesized as described earlier [39]. To obtain (4(((1*S*)-1-acetamido-1',2',3'-trimethoxy-6,7-dihydro-1*H*-benzo[5',6':5,4]cyclohepta[3,2-f]benzofuran-1-yl)methoxy)-4-oxobutanoic acid) **3**, sample **2** (50 mg, 0.12 mmol) and succinic anhydride (12 mg, 0.12 mmol) were dissolved in 2 ml of tetrahydrofuran under an inert atmosphere; then 17 µl of triethylamine (0.12 mmol) was added. The mixture was stirred for 2 h at 20°C and then 12 h at 70°C. After the reaction was completed (TLC control), the resulting solution was extracted with EtOAc, washed with brine and dried over Na₂SO₄. The solvent was removed under reduced pressure. The pure product **3** as white crystals (42 mg, 67%) was isolated by column chromatography, eluent petroleum spirit - ethyl acetate - ethanol (1:1:1). **¹H NMR** (400 MHz, CD₃OD): δ 8.60 (d, *J* = 8.0 Hz, 1H), 7.61 (s, 1H), 7.45 (s, 1H), 6.85 (s, 1H), 6.75 (s, 1H), 5.26 (s, 2H), 4.75 (dd, *J* = 11.6, 6.3 Hz, 1H), 3.89 (d, *J* = 5.6 Hz, 6H), 3.46 (s, 3H), 2.70 – 2.59 (m, 4H), 2.54 (dd, *J* = 12.3, 5.2 Hz, 1H), 2.34 – 2.20 (m, 2H), 2.04 (s, 3H), 1.94 (td, *J* = 11.5, 6.5 Hz, 1H). **¹³C NMR** (101 MHz, DMSO): δ 175.70, 172.96, 170.56, 154.64, 154.49, 153.52, 149.52, 147.79, 140.46, 134.85, 130.35, 128.77, 127.91, 127.30, 109.03, 107.01, 106.83, 60.65, 60.65, 57.43, 56.79, 51.37, 37.31, 31.23, 30.99, 30.10, 22.75. Both **3** and **4** were dissolved in DMSO and stored at -20°C.

Synthesis of furanoallocolchicinoid-chitosan conjugate

Conjugate **4** was synthesized from **3** and chitosan 40 kDa according to the published protocol [40]. Chitosan to **3** ratios were 1:5, 15 and 45. Chitosan (40 kDa, 52.1 mg, 0.001 mmol) was dissolved in 6 ml of distilled water, acidified with acetic acid to pH=6 and diluted with 15 ml of methanol, after which **3** (3.3, 10, or 30.0 mg (0.007, 0.02, or 0.059 mmol), EDC (45.3 mg, 0.236 mmol) and NHS (27.1 mg, 0.236 mmol) were added and the mixture was stirred for 24 h at room temperature. The resulting solution was dried under reduced pressure, washed with toluene, CH_2Cl_2 (5×50 ml) and dried in vacuo. The product was obtained as a pale-beige solid mass (78.2 mg). $^1\text{H NMR}$ (400 MHz, $\text{D}_2\text{O}:\text{TFA-d}_1 = 80:20$). Dry product was dissolved in phosphate buffered saline (PBS) at pH 7.2 and kept either at +4°C or frozen at -20°C until use.

Results and Discussion

Synthesis and characteristics of furanoallocolchicinoids

In the pilot experiments we have fulfilled an optimization of the compound **4** structure, namely, **3** was conjugated to chitosan with different MW (200, 40, and 12 kDa) and at different chitosan to **3** ratios (1:5, 1:15, 1:45). Conjugate with chitosan 200 kDa aggregated during storage; the activity of conjugate with chitosan 12 kDa was low possibly due to a relatively short backbone of chitosan molecule to immobilize several molecules of the compound **3**. Finally, chitosan with MW 40 kDa was used to obtain conjugate **4**.

The specific allocolchicinoid activity depended directly on the amount of immobilized groups (Figure S1, A-B). Concentration of **3** in **4** was determined by the comparison of IC₅₀ calculated from inhibitory titration curves obtained in Colo-357 and MiaPaCa-2 cell lines (Figure S1, C-D). As it was shown earlier [39] activity of the compound **2** was 5-10 times higher than of **1**, however the activity of the compound **3** containing -COOH group needed for chitosan conjugation, was comparable with colchicine **1** (Figure S1, C-D). Activity of conjugates **4** prepared at 1:5, 1:15, and 1:45 chitosan to **3** ratios were equivalent to 7, 160 and 1000 μM (Figure S1, E). The number of immobilized molecules of the compound **3** per chitosan molecule was 0.1, 1.3, and 7.5 accordingly (Figure S1, F). For all further *in vitro* and *in vivo* experiments the conjugate **4** at 1:45 ratio was used.

Scheme of synthesis, structures, NMR spectra and size distribution for the compounds **1-3** and *de novo* synthesized conjugate **4** are shown in Figure 1. Chitosan protons in NMR spectrum of the conjugate **4** interfered with the signals from **1-3** at <5 ppm (Figure 2), however peaks at >5 ppm were specific (shown with braces) for **1-3**.

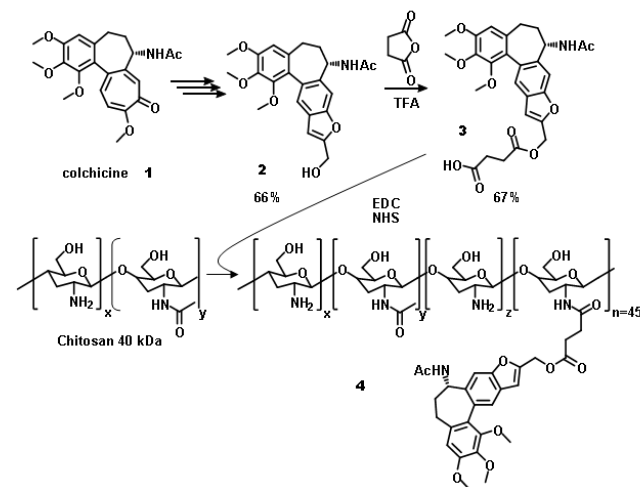


Figure 1: Scheme of synthesis. Structures of colchicine (**1**), furanoallocolchicinoids (**2-3**), and furanoallocolchicine-chitosan conjugate (**4**).

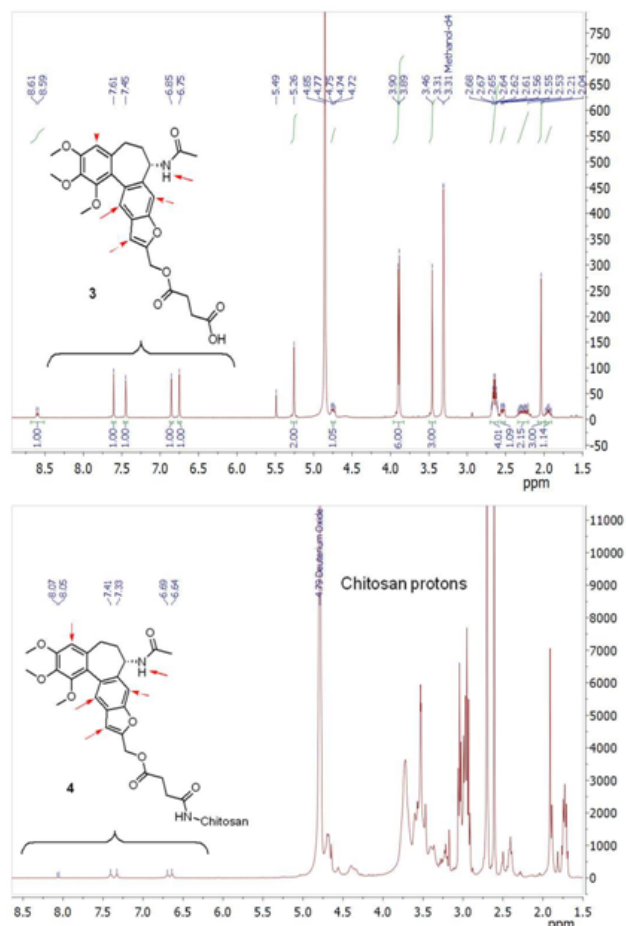


Figure 2: NMR spectra of furanoallocolchicine **3** (A) and furanocolchicine-chitosan conjugate **4** (B). Furanoallocolchicinoid specific peaks are shown with braces.

The size of **1-3** molecules was below the limit of DLS (<5 nm). Conjugation of **3** with chitosan at ratio 45 to 1 resulted in the size increase of **3** in at least up to 8 times. The sizes of chitosan and **4** molecules were determined by DLS and were comparable (28-40 nm). Unmodified chitosan, used to prepare **4**, could be dissolved only in diluted acids as its ζ -potential was +30 mV, while the conjugate **4** was not soluble at acidic pH and was dissolved in PBS at neutral pH. When measured, ζ -potential of **4** appeared to be -4 mV which was a result of chemical modifications. Negative ζ -potential of the drug used for IV injections is preferential as positively charged substances interact with negatively charged cells and thus are more toxic [43]. Besides, positively charged chitosan derivatives and chitosan based nanoparticles poorly penetrate cells than negatively charged ones [44].

Functional activity of **4** was determined as described above using 5 different cell lines including W1204, a Wnt-1 related murine epithelial cell line [42]. Activity of **1-3** is shown averaged for 5 cell lines (Figure 3A), and individual titration curves for **4** are shown with thin lines while averaged data are shown with a bold one (Figure 3B). As shown above, specific activity of **2** was higher than of colchicine **1** while its derivation with -COOH group decreased it to the colchicine one (Figure 3A). Functional activity of **4** was determined as 0.8 mM

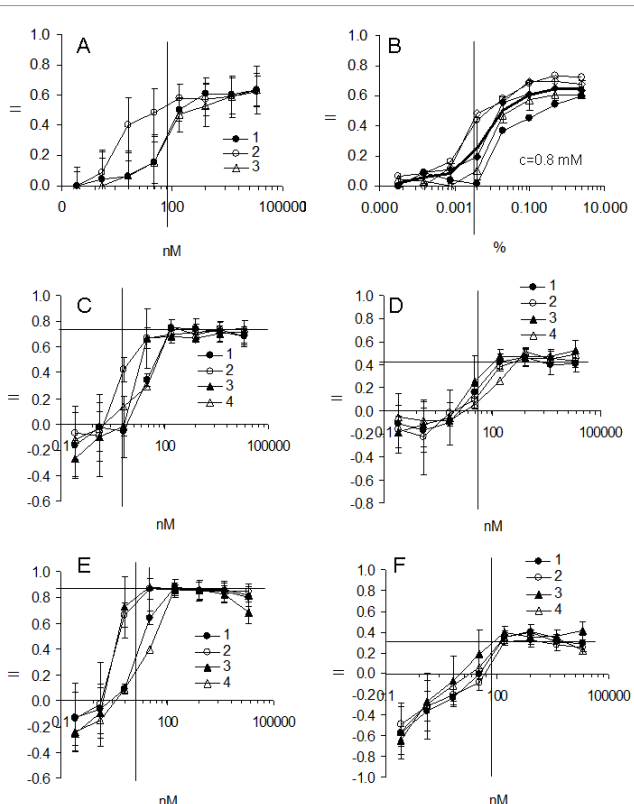


Figure 3: Effect of preparations **1-4** on cell proliferation. A. Inhibition of cell proliferation by **1-3**. Results are shown as average inhibitory indices (II) for the titration curves obtained for Colo-357, MiaPaca-2, HaCaT, EA.hy926, and W1203 cells. Vertical lines show IC_{50} values. B. Determination of effective furanoallocolchicinoid concentration in **4**. Compound **4** was titrated v/v and incubated with Colo-357, MiaPaca-2, HaCaT, EA.hy926, or W1204 cells (thin lines). Average inhibitory curve (bold line) was used to estimate IC_{50} for **4**. Final concentration of **3** in **4** was determined by comparison of IC_{50} 's for **3** and **4**. C-F. Colo-357 (C-D) and W1204 (E-F) were grown in 2D (C, E) and 3D (D, F) conditions. Preparations **1-4** in different concentrations were added onto preformed 2D or 3D cultures and incubated for 72 h. Results are shown as inhibitory indices. Horizontal lines show the plateau of the maximal inhibition values and vertical lines - IC_{50} for **4**.

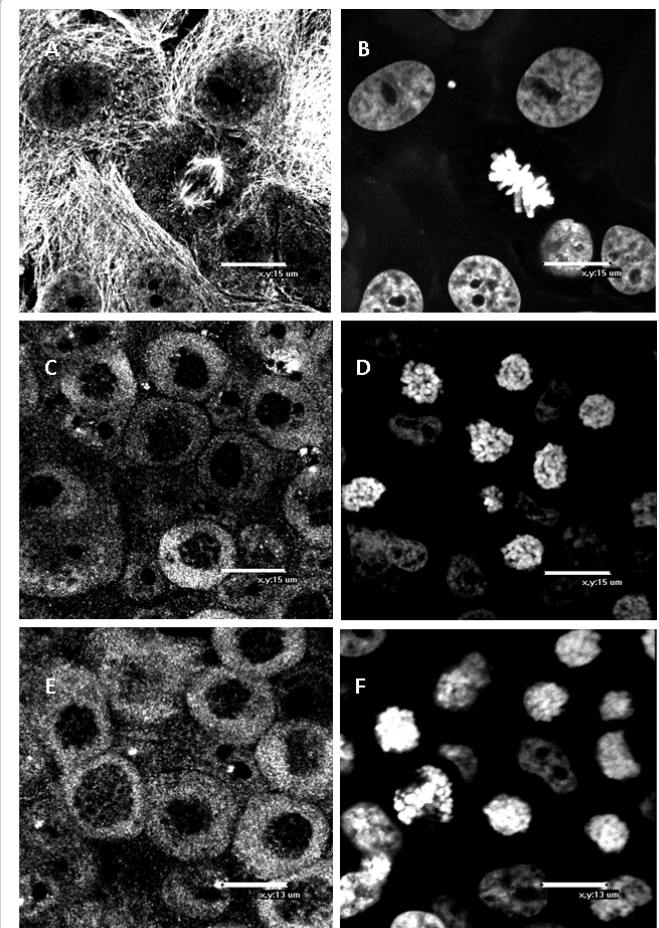


Figure 4: Effect of **3** and **4** on β -tubulin organization and nucleus structures in Colo-357 cells cultivated in 2D condition. Cells were seeded onto cover slips until adhesion. Compound **3** (C-D) and conjugate **4** (E-F) were added at 4 μ M for 72 h. Staining with anti- β -tubulin antibody (A, C, E) and Hoechst 33342 (B, D, F) in perforated cells in control (A-B) and treated (C-F) cultures. Scale bars correspond to 13-15 μ m.

which corresponded to 25 times dilution of **3** (20 mM) due to chitosan conjugation.

Functional activity of colchicinoids *in vitro*

Functional activity of **1-4** was tested in 2D and 3D cultures using human epithelial cell line Colo-357 and murine epithelial cell line W1204 (Figure 3), which originates from Wnt-1 breast tumor used in this study to estimate *in vivo* activity of furanoallocolchicinoid conjugate **4**. 3D cultures are believed to represent closer avascular *in vivo* tumors. Usually activity of antitumor drugs are lower in 3D cultures in comparison with 2D ones as it was shown for many antineoplastic drugs including antitubulins such as paclitaxel and vincristine [45]. However, 3D cultures were never tested to estimate sensitivity of cells to colchicinoids. The only publication on colchicine analogue E-combretastatin describes the penetration of the drug into 3D spheroids [46] while it does not compare cell sensitivity to the drug in 2D and 3D conditions. Thus, our data are the first study of colchicine, furanoallocolchicine and furanoallocolchicinoid-chitosan conjugate in 3D cultures.

Data for 2D and 3D cultures demonstrated that in both cases the cells were sensitive to **1-4** as was demonstrated by the dose-dependent curves. However, the cumulative cytostatic activity of **1-4** was 2-3 times

higher in 2D cultures (Figure 3C-F) as is evidenced by 80-90% maximal inhibition of cell proliferation in 2D cultures and only 30-40% - in 3D ones (Figure 3C-F, shown with horizontal lines). This was true both for human (Figure 3C-D) and murine (Figure 3E-F) cells. IC_{50} also was ~5 times higher in 3D cultures. This result can be explained by the activation of multidrug resistance transporter P-glycoprotein in 3D conditions absent in 2D conditions [47].

No difference in the activity was found between **1-4** in 3D cultures while the compound **2** was 5 times more active in 2D cultures as it was shown earlier [39].

Effects of the compound **3** and the conjugate **4** on β -tubulin organization was studied in 2D and 3D cultures in Colo-357 cells using confocal microscopy. The results are shown for β -tubulin organization (Figures 4 and 5, A, C, E) and nuclei structures (Figures 4 and 5, B, D, F). Both **3** and **4** disrupted tubulin microtubules and blocked mitotic spindle formation in 2D and 3D conditions.

Colchicine is also known and a vascular contacts disrupting agent [48,49]. Moreover, it was shown that the disruption of microtubules

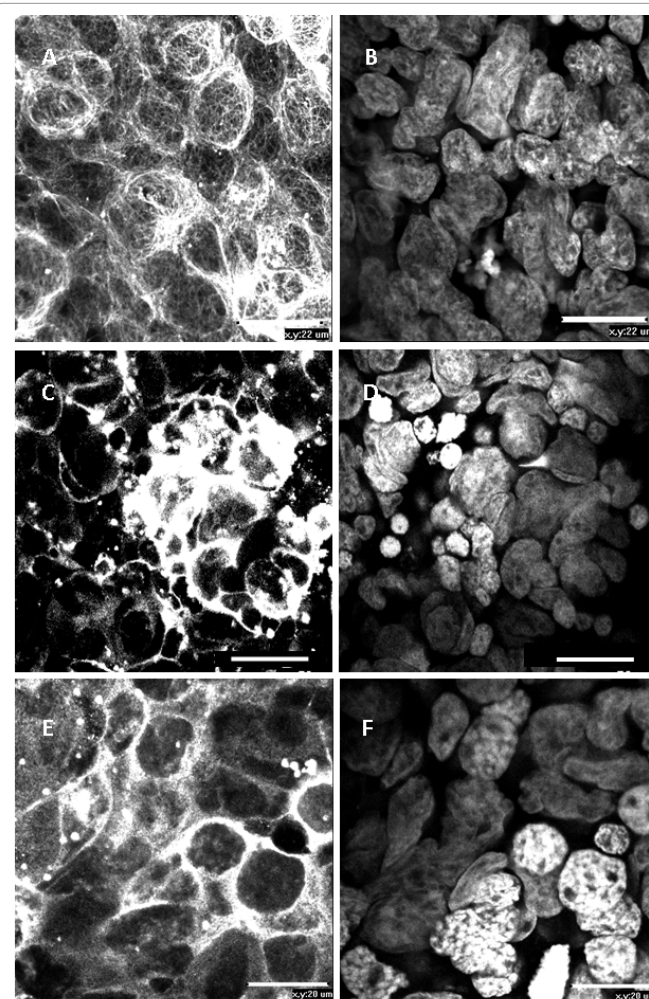


Figure 5: Effect of 3 and 4 on β -tubulin organization and nucleus structures in Colo-357 cells cultivated in 3D condition. Cells were seeded onto pHEMA treated 24-well plates until multicellular tumor spheroids were formed. Compound **3** (C-D) and conjugate **4** (E-F) were added at 4 μ M for 72 h. Spheroids were stained with anti- β -tubulin antibody (A, C, E) and Hoechst 33342 (B, D, F) in perforated cells, transferred onto cover slips and analyzed in control (A-B) and treated (C-F) cultures. Scale bar corresponds to 20-22 μ m.

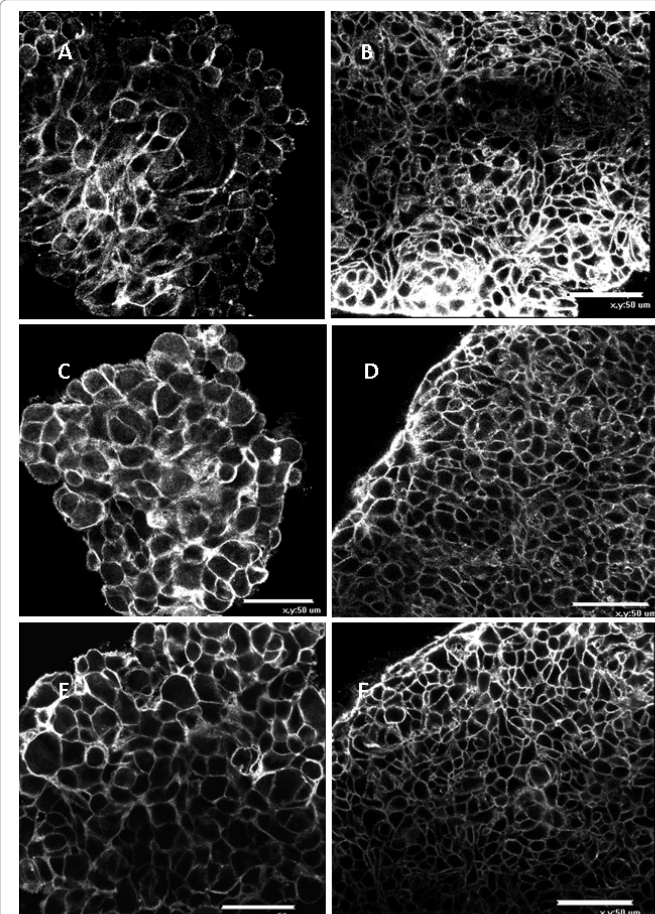


Figure 6: Effect of **3** and **4** on F-actin organization in epithelial and endothelial cells in 3D condition. Colo-357 (A, C, E) and EA.hy926 (B, D, F) cells were seeded onto pHEMA treated 24-well plates until multicellular tumor spheroids were formed. Compound **3** (C-D) and conjugate **4** (E-F) were added at 4 μ M for 72 h. Spheroids were stained with phalloidin-AlexaFluor499 in perforated cells, transferred onto cover slips and analyzed in control (A-B) and treated (C-F) cultures. Scale bar corresponds to 50 μ m.

with colchicine resulted in actin microfilament rearrangement in resting aortic endothelial monolayers [49]. To study whether it is true in epithelial in comparison with endothelial cells we also compared F-actin expression in 3D cultures after cell treatment with **3** and **4**. It appeared that F-actin expression and arrangement was unaffected by the compound **3** and the conjugate **4** in both types of cells (Figure 6).

One of the basic feature of colchicinoid action is a cell cycling suppression. Incubation of epithelial cells with the compounds **1**, **3**, and **4** induced cell accumulation in G2/M phase and a significant apoptosis both in 2D and 3D cultures (Figure 7). Of note, murine cells W1204 proliferated less in 3D conditions (Figure 7, I-J) and changed DNA condensation in G1 phase (note the shift of M2 fraction in treated versus control cells). Besides, the number of cells in S-phase was also increased (Figure 7, J, arrow).

Antitumor activity of furanoallocolchicinoids *in vivo*

Chitosan is a nontoxic polymer. It did not induce tubulin reorganization or cell cycle inhibition (Figure S2) however it could affect tumor growth. To exclude its effect, an additional control group treated with an equivalent amount of chitosan was included in the study. The results demonstrated that the conjugate **4** was significantly ($p<0.05$) more effective than the compound **2**, and both **2** and **4**

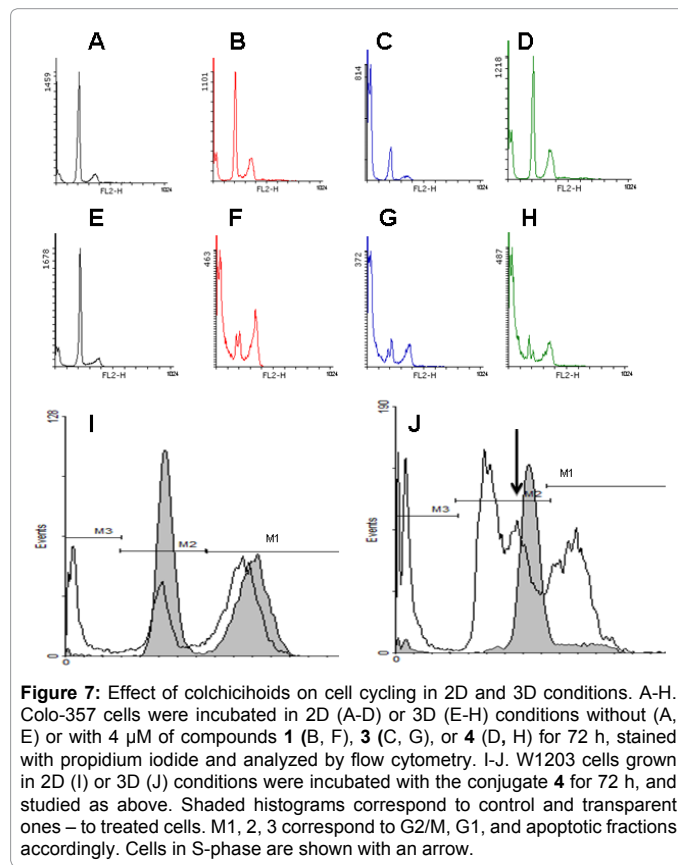


Figure 7: Effect of colchicinoids on cell cycling in 2D and 3D conditions. A-H. Colo-357 cells were incubated in 2D (A-D) or 3D (E-H) conditions without (A, E) or with 4 μ M of compounds 2 (B, F), 3 (C, G), or 4 (D, H) for 72 h, stained with propidium iodide and analyzed by flow cytometry. I-J. W1203 cells grown in 2D (I) or 3D (J) conditions were incubated with the conjugate 4 for 72 h, and studied as above. Shaded histograms correspond to control and transparent ones – to treated cells. M1, 2, 3 correspond to G2/M, G1, and apoptotic fractions accordingly. Cells in S-phase are shown with an arrow.

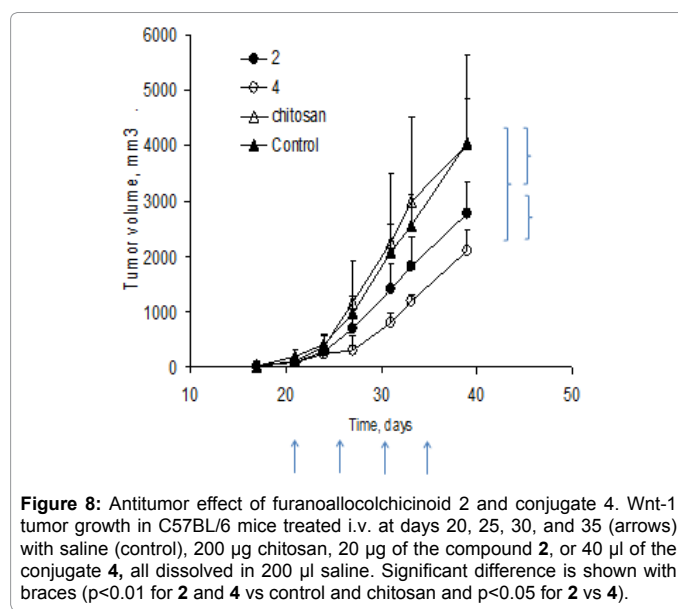


Figure 8: Antitumor effect of furanoallocolchicinoid 2 and conjugate 4. Wnt-1 tumor growth in C57BL/6 mice treated i.v. at days 20, 25, 30, and 35 (arrows) with saline (control), 200 μ g chitosan, 20 μ g of the compound 2, or 40 μ l of the conjugate 4, all dissolved in 200 μ l saline. Significant difference is shown with braces ($p<0.01$ for 2 and 4 vs control and chitosan and $p<0.05$ for 2 vs 4).

significantly inhibited the tumor growth in comparison with the control and chitosan groups (Figure 8).

Conclusion

The results of this study demonstrated that the decoration of small hydrophobic molecules could serve several important purposes: it makes the drug less lipophilic, increases the molecule size, shields the drugs from the instant contact with blood cells, and possibly decreases

drug accumulation in non-target organs, resulting in an improved antitumor efficacy and possibly few side effects. These findings are in a good agreement with earlier published data [28-35]. Although in this work we did not study the biodistribution of 3 and 4 in tumor and non-target organs, the results of other groups show that conjugates of a small size such as antibody-drug ones demonstrate the same biodistribution as an antibody alone [50], while nanosized carrier accumulated better in the tumor than in non-target organs [51].

The polymers often used to decorate active substances such as PEG, PLA, liposomes, in many cases lack multiple reactive groups needed to load them with several moieties by this limiting the functional activities of the conjugates [33]. Among few biocompatible polymers possessing multiple reactive groups, chitosan is one of the best candidates for the development of drug delivery systems. Modernly chitosan is used in medicine with no side effects as wound healing films, hemostatic sponges, and hydrogels for regenerative medicine [52,53]. The obstacle in a wider clinical application of chitosan is its poorly standardized structure. Due to the availability of multiple reactive groups, chitosan interacts with its own side chains and plasma proteins via electrostatic, hydrophobic, Van-Der-Waals forces and hydrogen bonds [54]. This makes chitosan a flexible molecule. We showed that a direct conjugation of 3 to chitosan did not affect specific colchicine activity. Thus, no special degradable linkers were required. Taken into account rather simple synthesis of furanoallocolchicinoids 2 and 3, unlimited renewable sources and cheap production of chitosan, colchicine-chitosan conjugates can be considered as highly perspective medications for cancer treatment.

Conflict of Interest

There are no financial or other issues that might lead to conflict of interest.

Acknowledgements

This work was supported by the Russian Scientific Fund, project #16-13-10248 and by Russian Federation President Scholarships donated to A.A. Zubareva (# 1386.2015.4).

References

- Stec-Martyna E, Ponassi M, Miele M, Parodi S, Felli L, et al. (2012) Structural comparison of the interaction of tubulin with various ligands affecting microtubule dynamics. *Curr Cancer Drug Targets* 12: 658-666.
- Seligmann J, Twelves C (2013) Tubulin: an example of targeted chemotherapy. *Future Med Chem* 5: 339-352.
- Cortes J, Vidal M (2012) Beyond taxanes: the next generation of microtubule-targeting agents. *Breast Cancer Res Treat* 133: 821-830.
- Katsetos CD, Dráber P (2012) Tubulins as therapeutic targets in cancer: from bench to bedside. *Curr Pharm Des* 18: 2778-2792.
- Cerquaglia C, Diaco M, Nucera G, La Regina M, Montalto M, et al. (2005) Pharmacological and clinical basis of treatment of Familial Mediterranean Fever (FMF) with colchicine or analogues: an update. *Curr Drug Targets Inflamm Allergy* 4: 117-124.
- Masuda K, Nakajima A, Urayama A, Nakae K, Kogure M, et al. (1989) Double-masked trial of cyclosporin versus colchicine and long-term open study of cyclosporin in Behcet's disease. *Lancet* 1: 1093-1096.
- Imazio M, Bobbio M, Cecchi E, Demarie D, Pomari F, et al. (2005) Colchicine as first-choice therapy for recurrent pericarditis: results of the CORE (COlchicine for REcurrent pericarditis) trial. *Archives of internal medicine* 165: 1987-1991.
- Imazio M, Brucato A, Cemin R, Ferrua S, Belli R, et al. (2011) Colchicine for recurrent pericarditis (CORP): a randomized trial. *Ann Intern Med* 155: 409-414.
- Cocco G, Chu DC, Pandolfi S (2010) Colchicine in clinical medicine. A guide for internists. *Eur J Intern Med* 21: 503-508.

10. Finkelstein Y, Aks SE, Hutson JR, Juurlink DN, Nguyen P, et al. (2010) Colchicine poisoning: the dark side of an ancient drug. *Clin Toxicol (Phila)* 48: 407-414.
11. Dickinson M, Juneja S (2009) Haematological toxicity of colchicine. *Br J Haematol* 146: 465.
12. Swain SM, Arezzo JC (2008) Neuropathy associated with microtubule inhibitors: diagnosis, incidence, and management. *Clin Adv Hematol Oncol* 6: 455-467.
13. Fang KM, Liu JJ, Li CC, Cheng CC (2015) Colchicine derivative as a potential anti-glioma compound. *J Neurooncol* 124: 403-412.
14. Kunischner LJ, Fine H, Hess K, Jaeckle K, Kyritsis AP, et al. (2002) CI-980 for the treatment of recurrent or progressive malignant gliomas: national central nervous system consortium phase I-II evaluation of CI-980. *Cancer Invest* 20: 948-954.
15. Tsimerman AM, Akerley W, Schabel MC, Hong DS, Uehara C, et al. (2010) Phase I clinical trial of MPC-6827 (Azixa), a microtubule destabilizing agent, in patients with advanced cancer. *Mol. Cancer. Ther* 9: 3410-3419.
16. Nepali K, Ojha R, Lee HY, Liou JP (2016) Early investigational tubulin inhibitors as novel cancer therapeutics. *Expert Opin Investig Drugs* 25: 917-936.
17. Vindya NG, Sharma N, Yadav M, Ethiraj KR (2015) Tubulins - the target for anticancer therapy. *Curr Top Med Chem* 15: 73-82.
18. Sabouraud A, Chappay O, Dupin T, Scherrmann JM (1994) Binding of colchicine and thiocolchicoside to human serum proteins and blood cells. *Int J Clin Pharmacol Ther* 32: 429-432.
19. Chappay ON, Niel E, Wautier JL, Hung PP, Dervichian M (1993) Colchicine disposition in human leukocytes after single and multiple oral administration. *Clinical Pharmacology & Therapeutics* 54: 360-7.
20. Satpathi D, Korde A, Kothari K, Sarma HD, Venkatesh M, et al. (2008) Preparation and in-vivo evaluation of (188)Re(CO)(3)-colchicine complex for use as tumor-targeting agent. *Cancer Biother Radiopharm* 23: 741-748.
21. Mehta BM, Levchenko A, Rosa E, Kim SW, Winnick S, et al. (1996) Evaluation of Carbon-14-Colchicine Biodistribution with Whole-body Quantitative Autoradiography in. *J Nucl Med* 37: 312-314.
22. Erfani M, Shamsaei M, Mohammadbagheri F, Shirmardi SP (2014) Synthesis and evaluation of a 99mTc-labeled tubulin-binding agent for tumor imaging. *J Labelled Comp Radiopharm* 57: 419-424.
23. Colby AH, Liu R, Schulz MD, Padera RF, Colson YL, et al. (2016) Two-step delivery: exploiting the partition coefficient concept to increase intratumoral paclitaxel concentrations in vivo using responsive nanoparticles. *Scientific reports* 6.
24. Ediriwickrema A, Saltzman WM (2015) Nanotherapy for Cancer: Targeting and Multifunctionality in the Future of Cancer Therapies. *ACS Biomater Sci Eng* 1: 64-78.
25. Crielaard BJ, van der Wal S, Lammers T, Le HT, Hennink WE, et al. (2011) A polymeric colchicinoid prodrug with reduced toxicity and improved efficacy for vascular disruption in cancer therapy. *Int. J. Nanomedicine* 6: 2697-2703.
26. Matsumura Y, Maeda H (1986) A new concept for macromolecular therapeutics in cancer chemotherapy: mechanism of tumorotropic accumulation of proteins and the antitumor agent smancs. *Cancer research* 46: 6387-6392.
27. Ringsdorf H (1975) Structure and properties of pharmacologically active polymers. *Journal of Polymer Science: Polymer Symposia* 51: 135-153.
28. Parveen S, Sahoo SK (2006) Nanomedicine: clinical applications of polyethylene glycol conjugated proteins and drugs. *Clin Pharmacokinet* 45: 965-988.
29. Larson N, Ghandehari H (2012) Polymeric conjugates for drug delivery. *Chem Mater* 24: 840-853.
30. Greenwald RB, Pendri A, Bolikal D, Gilbert CW (1994) Highly water soluble taxol derivatives: 2'-polyethyleneglycol esters as potential prodrugs. *Bioorganic & Medicinal Chemistry Letters*. 4: 2465-70.
31. Greenwald RB, Choe YH, McGuire J, Conover CD (2003) Effective drug delivery by PEGylated drug conjugates. *Adv Drug Deliv Rev* 55: 217-250.
32. Denny WA (2004) Tumor-activated prodrugs--a new approach to cancer therapy. *Cancer Invest* 22: 604-619.
33. Hawkins MJ, Soon-Shiong P, Desai N (2008) Protein nanoparticles as drug carriers in clinical medicine. *Adv Drug Deliv Rev* 60: 876-885.
34. Kamal A, Kumar GB, Vishnuvardhan MV, Shaik AB, Reddy VS, et al. (2015) Synthesis of phenstatin/isocombretastatin-chalcone conjugates as potent tubulin polymerization inhibitors and mitochondrial apoptotic inducers. *Organic & biomolecular chemistry* 13: 3963-3981.
35. Bagnato JD, Eilers AL, Horton RA, Grissom CB (2004) Synthesis and characterization of a cobalamin-colchicine conjugate as a novel tumor-targeted cytotoxin. *J Org Chem* 69: 8987-8996.
36. Ngo DH, Vo TS, Ngo DN, Kang KH, Je JY, et al. (2015) Biological effects of chitosan and its derivatives. *Food Hydrocolloids* 51: 200-216.
37. Mourya VK, Inamdar NN (2008) Reactive & Functional Polymers Chitosan-modifications and applications. *Opportunities galore* 68: 1013-1051.
38. Jain A, Gulbake A, Shilpi S, Jain A, Hurkat P, et al. (2013) A new horizon in modifications of chitosan: syntheses and applications. *Crit Rev Ther Drug Carrier Syst* 30: 91-181.
39. Voitovich YV, Shegravina ES, Sitnikov NS, Faerman VI, Fokin VV, et al. (2015) Synthesis and biological evaluation of furanoallocolchicinoids. *J Med Chem* 58: 692-704.
40. Mathiyalagan R, Subramaniyam S, Kim YJ, Kim YC, Yang DC (2014) Ginsenoside compound K-bearing glycol chitosan conjugates: synthesis, physicochemical characterization, and in vitro biological studies. *Carbohydrate polymers* 112: 359-366.
41. Denizot F, Lang R (1986) Rapid colorimetric assay for cell growth and survival. Modifications to the tetrazolium dye procedure giving improved sensitivity and reliability. *J Immunol Methods* 89: 271-277.
42. Svirshchevskaya EV, Mariotti J, Wright MH, Viskova NY, Telford W, et al. (2008) Rapamycin delays growth of Wnt-1 tumors in spite of suppression of host immunity. *BMC Cancer* 8: 176.
43. Luong D, Kesharwani P, Deshmukh R, Amin MC, Gupta U, et al. (2016) PEGylated PAMAM dendrimers: Enhancing efficacy and mitigating toxicity for effective anticancer drug and gene delivery. *Acta Biomaterialia* 43: 14-29.
44. Zubareva AA, Shcherbinina TS, Varlamov VP, Svirshchevskaya EV (2015) Intracellular sorting of differently charged chitosan derivatives and chitosan-based nanoparticles. *Nanoscale* 7: 7942-7952.
45. Villaverde MS, Gil-Cardeza ML, Glikin GC, Finocchiaro LM (2012) Interferon- β lipofection I. Increased efficacy of chemotherapeutic drugs on human tumor cells derived monolayers and spheroids. *Cancer gene therapy* 19: 508-516.
46. Scherer KM, Bisby RH, Botchway SW, Hadfield JA, Haycock JW, et al. (2015) Three-dimensional imaging and uptake of the anticancer drug combretastatin in cell spheroids and photoisomerization in gels with multiphoton excitation. *Journal of biomedical optics* 20: 078003.
47. Xing H, Gao QL, Yang XK, Li J, Gao C, et al. (2003) Resistance of multicellular spheroids to taxol in human ovarian cancer and its mechanism. *Ai Zheng* 22: 826-830.
48. Canelo MD, Noppen S, Bueno O, Prota AE, Bargsten K, et al. (2016) Antivascular and antitumor properties of the tubulin-binding chalcone TUB091. *Oncotarget*
49. Lee JS, Gotlieb AI (2005) Microtubules regulate aortic endothelial cell actin microfilament reorganization in intact and repairing monolayers.
50. Giddabasappa A, Gupta VR, Norberg R, Gupta P, Spilker ME, et al. (2016) Biodistribution and Targeting of Anti-5T4 Antibody-Drug Conjugate Using Fluorescence Molecular Tomography. *Molecular Cancer Therapeutics*.
51. Tran PH, Tran TT, Lee BJ (2014) Biodistribution and pharmacokinetics in rats and antitumor effect in various types of tumor-bearing mice of novel self-assembled gelatin-oleic acid nanoparticles containing paclitaxel. *Journal of biomedical nanotechnology* 10: 154-165.
52. Ahmed TA, Aljaeid BM (2016) Preparation, characterization, and potential application of chitosan, chitosan derivatives, and chitosan metal nanoparticles in pharmaceutical drug delivery. *Drug design, development and therapy* 10: 483.
53. Swierczewska M, Han HS, Kim K, Park JH, Lee S (2016) Polysaccharide-based nanoparticles for theranostic nanomedicine. *Adv Drug Deliv Rev* 99: 70-84.
54. Aggarwal P, Hall JB, McLeland CB, Dobrovolskaia MA, McNeil SE (2009) Nanoparticle interaction with plasma proteins as it relates to particle biodistribution, biocompatibility and therapeutic efficacy. *Advanced drug delivery reviews* 61: 428-437.